Observation of Pontecorvo reactions with open strangeness: $\overline{\mathrm{p}}\mathrm{d}\to\Lambda\mathrm{K}^0$ and $\overline{\mathrm{p}}\mathrm{d}\to\Sigma^0\mathrm{K}^0$

The Crystal Barrel Collaboration

A. Abele [h], J. Adomeit [g], C. Amsler [o], C.A. Baker [e], B.M. Barnett [c,1], C.J. Batty [e], M. Benayoun [ℓ], A. Berdoz [m], S. Bischoff [h], P. Blüm [h], K. Braune [k], D.V. Bugg [i], T. Case [a], O. Cramer [k], K.M. Crowe [a], T. Degener [b], N. Djaoshvili [f], M. Doser [f], W. Dünnweber [k], D. Engelhardt [h], M.A. Faessler [k], P. Giarritta [o], R.P. Haddock [j], F.H. Heinsius [a,2], M. Heinzelmann [o], A. Herbstrith [h], M. Herz [c], N.P. Hessey [k], P. Hidas [d], C. Hodd [i], C. Holtzhaußen [h], D. Jamnik [k,3], H. Kalinowsky [c], P. Kammel [a], J. Kisiel [f,4], E. Klempt [c], H. Koch [b], M. Kunze [b], U. Kurilla [b], M. Lakata [a], R. Landua [f], H. Matthäy [b], R. McCrady [m], J. Meier [g], C.A. Meyer [m], L. Montanet [f], R. Ouared [g], K. Peters [b], B. Pick [c], M. Ratajczak [b], C. Regenfus [o,8], W. Roethel [k], R. Seibert [g], S. Spanier [o,5], H. Stöck [b], C. Straßburger [c], U. Strohbusch [g], M. Suffert [n], J.S. Suh [c], U. Thoma [c], M. Tischhäuser [h], I. Uman [k], C. Völcker [k], S. Wallis-Plachner [k], D. Walther [k,6], U. Wiedner [k,7], K. Wittmack [c], B.S. Zou [i], Č. Zupančič [k]

[a] *University of California, LBNL, Berkeley, CA 94720, USA*

[b] *Universität Bochum, D-44780 Bochum, FRG*

[c] *Universität Bonn, D-53115 Bonn, FRG*

[d] *Academy of Science, H-1525 Budapest, Hungary*

[e] *Rutherford Appleton Laboratory, Chilton, Didcot OX11 0QX, UK*

[f] *CERN, CH-1211 Geneva 4, Switzerland*

[g] *Universität Hamburg, D-22761 Hamburg, FRG*

[h] *Universität Karlsruhe, D-76021 Karlsruhe, FRG*

[i] *Queen Mary and Westfield College, London E1 4NS, UK*

[j] *University of California, Los Angeles, CA 90024, USA*

[k] *Universität München, D-80333 München, FRG*

[ℓ] *LPNHE Paris VI, VII, F-75252 Paris, France*

Preprint submitted to Elsevier Preprint *10 September 1999*

[m] *Carnegie Mellon University, Pittsburgh, PA 15213, USA*
[n] *Centre de Recherches Nucléaires,F-67037 Strasbourg, France*
[o] *Universität Zürich, CH-8057 Zürich, Switzerland*

Abstract

We report the first observation of antiproton annihilation on the deuteron into two-body channels with open strangeness. These reactions are of the Pontecorvo type, designating annihilations kinematically not possible on a free nucleon. With antiprotons stopped in a liquid deuterium target, a $\mathrm{K^0_S}$ - and Λ - enriched sample of events, corresponding to about 10^9 annihilations, was recorded with the Crystal Barrel experiment, using a Silicon microstrip detector for triggering on secondary decays. The final states $\Lambda\mathrm{K^0_S}$ and $\Sigma^0\mathrm{K^0_S}$, with $\Sigma^0\to\Lambda\gamma$, $\Lambda\to\mathrm{p}\pi^-$, $\mathrm{K^0_S}\to\pi^+\pi^-$, and the equivalent final states $\Lambda\mathrm{K^0_L}$ and $\Sigma^0\mathrm{K^0_L}$, with noninteracting $\mathrm{K^0_L}$, were identified. The $\overline{\mathrm{p}}\mathrm{d}$ branching fraction into $\Lambda\mathrm{K^0}$ and $\Sigma^0\mathrm{K^0}$ are $(2.35 \pm 0.45) \times 10^{-6}$ and $(2.15 \pm 0.45) \times 10^{-6}$, respectively. This similarity disagrees strongly with two-step model predictions and supports the statistical (fireball) model.

Annihilation reactions of antinucleons on atomic nuclei that demand the participation of more than one nucleon were envisaged by Pontecorvo [1] shortly after the discovery of the antiproton. By energy and momentum conservation, these so-called Pontecorvo reactions cannot occur on a free nucleon. Antiproton annihilation on the deuteron into a single meson and a baryon is the prime example, elaborated in a variety of theoretical papers (see, e.g.[2-7]).

Experimentally, only a few $\overline{\mathrm{p}}\mathrm{d}$ Pontecorvo channels have been clearly identified: $\mathrm{p}\pi^-$ [8,9], $\mathrm{n}\pi^0$, $\mathrm{n}\eta$, $\mathrm{n}\omega$ [10] and $\Delta^{0/+}(1232)\pi^{0/-}$ [11]. The branching ratios of $\overline{\mathrm{p}}\mathrm{d}$ (at rest) into these channels, in the range (0.3-3.0) $\times10^{-5}$, did not allow a distinctive evaluation of the different theoretical approaches.

The models fall into two classes using either the two-step or the fireball picture, which are extremes with respect to the involved degrees of freedom. The former [2-4] assumes annihilation of the antiproton on one of the nucleons in the deuteron into a pair of mesons and subsequent absorption of one of them on the other nucleon. The intermediate meson is highly virtual. The latter model

[1] Now at University of Mainz, Mainz, Germany
[2] Now at University of Freiburg, Freiburg,Germany
[3] University of Ljubljana, Ljubljana, Slovenia
[4] University of Silesia, Katowice, Poland
[5] Now at SLAC, Stanford, USA
[6] Now at University of Bonn, Bonn, Germany
[7] Now at Uppsala University, Uppsala, Sweden
[8] This work is part of the PhD thesis of C. Regenfus at the University of Munich

[5,6] pictures a compound system ('fireball') formed by the participating 3 antiquarks and 6 quarks decaying statistically. The Regge model was suggested as an approach intermediate between these extremes [7].

The study of Pontecorvo reactions with open strangeness was often proposed [2,4,6-10] since strangeness production is expected to probe quark dynamics. Two-step calculations predict branching ratios orders of magnitude lower than fireball calculations. For the lowest mass channels, ΛK^0 and $\Sigma^{0/-}K^{0/+}$, the former yield values of a few 10^{-7} and 10^{-9}, respectively, whereas the latter lead to rather similar values in the 10^{-6} range. The ratio of these two branching fractions is considered to be fairly independent of model parameters in both approaches. The large difference of the two-step branching fractions arises from different coupling strengths in the absorption of the intermediate $\overline{K}$ meson. The $KN\Lambda$ coupling is well known [12] to be enhanced with respect to $KN\Sigma$. In contrast, the statistical weights of ΣK and ΛK^0, which are crucial for the fireball decay, give a ratio of almost 3:1 (1:1 if only the neutral combination $\Sigma^0 K^0$ is taken into account).

In this Letter we report the observation of Pontecorvo reactions with open strangeness. The $\overline{p}d$ annihilation channels ΛK^0 and $\Sigma^0 K^0$ are identified for both modes of the neutral K meson, K^0_L and K^0_S. The $\overline{p}d$ branching ratios are extracted independently for both modes, yielding consistent results.

The experiment was carried out with the Crystal Barrel detector [13] using antiprotons of 200 MeV/c from the LEAR facility at CERN. The beam with a typical intensity of 5 to 10 kHz was stopped in a liquid deuterium target in the centre of the detector. Charged particle momenta were measured with a cylindrical drift chamber in a magnetic field of 1.5 T parallel to the incident beam. The differential energy loss in the drift chamber was used to separate protons from pions. Photons were detected with 1380 CsI (Tl) crystals in a barrel-shape arrangement surrounding the drift chamber and covering 98% of 4π. The non-interaction probability of K^0_L in the barrel is about 50 % for momenta above 200 MeV/c.

A cylindrical Silicon microstrip detector (SVX) was used to provide efficient triggering on secondary vertices [14,15], replacing the two-layer proportional chamber of the original set-up [13]. It consists of 15 partly overlapping microstrip modules surrounding the target at a mean radius of 14 mm. Ranging from 15° to 145° in polar angle (with respect to the beam axis) the SVX fully covered the solid angle of the drift chamber. An additional segmented Silicon diode was placed directly in front of the target entrance, inside the SVX, to supply the $\overline{p}$-stop trigger. Charged-particle multiplicities were derived from the strip sides and the nonsegmented backplanes of the SVX modules. A fast topological trigger ($4\,\mu$s) required a multiplicity increase between the latter and the surrounding drift chamber. This trigger was used for recording the present data with either one or two secondary vertices, corresponding to a multiplicity increase from 0 to 2 for ΛK^0_L and $\Sigma^0 K^0_L$ or from 0 to 4 for ΛK^0_S and $\Sigma^0 K^0_S$ events, respectively.

An example from the event display is shown in Fig. 1. Two secondary vertices outside the SVX are traced in the hit pattern of the drift chamber. An isolated photon entry is found in the crystals in addition to energy deposits matching the tracks of charged particles. Full reconstruction identifies this event as being of the Pontecorvo type $\Sigma^0 K^0$ with successive $\Sigma^0 \to \Lambda\gamma$, $\Lambda \to p\pi^-$ and $K^0_S \to \pi^+\pi^-$ decays.

Samples of about 10^6 events each were recorded with the 2- and 4-prong topological triggers, which were employed in parallel. Both triggers enrich the present Pontecorvo channels by roughly two orders of magnitude with respect to a minimum bias experiment. These data sets were analysed separately to obtain independent evidence and branching ratios for the K^0_L and for the K^0_S modes of the Pontecorvo channels. Both samples were cleaned up off-line by requiring unambiguous single or double vertex fits for 2 or 4 reconstructed charged particles, respectively, with pairwise opposite charges. The vertex position was required to agree with the geometry defined by the interaction point and the detector set-up. Events containing γ conversions into e^+e^- did not pass the subsequent selection steps. Backscattered charged particles from the calorimeter were eliminated by a cut requiring an upper limit of 162° for the opening angle at a vertex, in accord with the much smaller maximum opening angles allowed by kinematics for the reactions of interest. The resulting 2- and 4-prong samples, (A) and (B), consist of 5×10^5 and 6×10^4 events, respectively, and their analyses will be outlined in turn.

Entries in the crystal barrel, not matching charged particle trajectories, are identified as photons, if the energy deposit in the centre crystal of a local maximum amounts to more than 13 MeV, if at least 4 % of the cluster energy is distributed over adjacent crystals, and if the cluster is not recognised as "split-off" from charged particles or other photons [13].

While the majority of events in sample (A) is of the type $K^0\overline{K^0}\,k\pi^0$ (k=0,1,2,...) with a spectator neutron, a fraction of 10 % contains $\Lambda \to p\pi^-$ decays. This fraction is selected by imposing a broad ($10\,\sigma$) window on the Λ peak in the invariant mass spectrum (see below and [15]) of the two charged particles which are identified as p and π^- by means of their differential energy losses dE/dx. These events are displayed in Fig. 2a where the total energy deposit from photons in the calorimeter (ESUM) is plotted versus the modulus of the sum of both charged particle momenta at their vertex. The three dominant broad bands can be attributed, from bottom to top, to $\Lambda K^0\,k\pi^0$ reactions with a noninteracting K^0_L, an interacting K^0_L and a $K^0_S \to \pi^0\pi^0$ decay. Two further event groupings with zero photon energy are discernible, one of which contains $K^0_S\,(\to\pi^+\pi^-)$ K^0_L(noninteracting) $n_{spectator}$ background events surviving the above, rather generous cuts. The other group is centered at a momentum of 1100 MeV/c, fulfilling the ΛK^0 two-body kinematics. Hence, by virtue of the hermeticity of the crystal barrel calorimeter, evidence for this annihilation channel is obtained already at this selection stage.

A subset of the events in Fig. 2a contains $\Sigma^0\to\Lambda\gamma$ decays. These are selected by imposing a broad window ($10\,\sigma$) on the Σ^0 peak in the invariant mass spectrum (see below and [15]) of all $\Lambda\gamma$ combinations of each event. For their representation in a plot of calorimeter energy versus Σ^0 momentum (Fig. 2b), the photon attributed to Σ^0 decay is not taken into account in ESUM but included in the Σ^0 momentum. In a similar fashion as above, a group of $\Sigma^0 K^0_L$ events is discernible at ESUM = 0, already at this stage of preselection.

Possible biases in particle identification by dE/dx were checked by replacing the above p/π^+ discrimination by a broad ($10\,\sigma$) window on the proton branch only and by imposing no cuts on the other charged particle. No significant changes occurred in the regions of interest in Figs. 2a and b.

Two cuts are applied to the preselected event samples to reduce background. First, ESUM = 0 is required, i.e. no photon or no residual photon according to Figs. 2a and b, respectively. Second, an upper limit is set for the $p\pi^-$ opening angle. In the opening angle versus momentum distributions, shown in Figs. 3a and 3b, the $\Lambda\to p\pi^-$ decay is well separated from the $K^0_S\to\pi^+\pi^-$ decay in the background noticed above. Cuts according to the largest possible $p\pi^-$ opening angle, allowed by kinematics for ΛK^0 ($\Lambda\to p\pi^-$) and $\Sigma^0 K^0$ ($\Sigma^0\to\Lambda\gamma$, $\Lambda\to p\pi^-$), were applied as indicated in Fig. 3.

The final selection was performed in the invariant mass versus momentum distributions shown in Figs. 4a and b. Well-defined Λ and Σ^0 peaks are obtained in the projected invariant mass spectra, and the momentum spectra show corresponding peaks at momentum values consistent with the $\overline{p}d\to$ hyperon + kaon two-body kinematics. The background below the peaks is rather small. It is worth pointing out that no kinematic fitting was required for this selection. Guided by Monte Carlo calculations, windows were set as indicated, containing 113 ΛK^0_L and 92 $\Sigma^0 K^0_L$ candidates, respectively.

Background contributions from other channels were estimated by means of Monte Carlo simulations using relative intensities extracted from the present data. Feed-through from $\Sigma^0 K^0_L$ to ΛK^0_L events, due to an unidentified photon from the Σ^0 decay, is calculated to be centered at a Λ momentum of 920 MeV/c. Its intensity is in accordance with the weak accumulation of events on the left side of the box in Fig. 4a. The calculated contribution to the sample in the box amounts to only 3 events. A similar estimate is obtained for background from $\Lambda K^0_L\pi^0$ events with undetected π^0. Background from misidentified $K_S^0 K_L^0 n_{spectator}$ events is found to be negligible. Feed-through from $\Lambda K_L^0 \pi^0$, where only one of the π^0 decay photons is not detected, represents the most significant background in the $\Sigma^0 K_L^0$ sample (Fig. 4b). It is calculated to be spread over a large range with relative intensity in accordance with the observed diffuse background. The final event numbers given in Table 1 were corrected for these background contributions. The systematic error on the number of events is taken to be equal to the number of background events.

Independent evidence for the same annihilation reactions, but with secondary charged K_S^0 decay, is provided by the 4-prong data sample (B). In this case both reaction products can be reconstructed separately. Candidate events of type a) ΛK_S^0 ($\Lambda \rightarrow p\pi^-$, $K_S^0 \rightarrow \pi^+\pi^-$) and b) $\Sigma^0 K_S^0$ ($\Sigma^0 \rightarrow \Lambda\gamma$, $\Lambda \rightarrow p\pi^-$, $K_S^0 \rightarrow \pi^+\pi^-$) are selected by dE/dx identification of the pions and protons and by $10\,\sigma$ windows centered on the K_S^0 and Λ peaks in the invariant $\pi^+\pi^-$ and $p\pi^-$ masses, respectively. Again, zero or one photon is required for type a) or b) events, respectively, and a broad ($10\,\sigma$) window around the Σ^0 mass is applied to the $\Lambda\gamma$ invariant mass in the latter case. Opening angles for Λ decay are restricted to the same ranges as above (see Figs. 3a, b) and additional cuts were applied to the K_S^0 decay opening angle and to the angle between the primary K_S^0 and Λ (respectively Σ^0) momentum vectors ($> 174°$). Background suppression by the threefold cuts on opening angles is very efficient. Two-dimensional representations of momentum versus momentum and invariant mass versus invariant mass are shown in Figs. 5a-d. Intensity maxima at the correct identical momentum values and at the respective masses (see insets) give evidence for the Pontecorvo channels. The peak contents are also given in Table 1. Background contributions were estimated from the intensity distributions in Figs. 5b, d and used to evaluate the systematic errors, as above.

Annihilation rates of $\overline{p}d$ at rest into the observed channels were deduced by normalising to the yields of reactions with the same trigger topologies:

(i) $\overline{p}d \rightarrow K_S^0\,(\rightarrow \pi^+\pi^-)\ K_L^0$(noninteracting) $n_{spectator}$ in the two-prong case, and

(ii) $\overline{p}d \rightarrow K_S^0\,(\rightarrow \pi^+\pi^-)\ K_S^0\,(\rightarrow \pi^+\pi^-)\ n_{spectator}$ in the four-prong case.

In bubble chamber experiments [16] the rates of $(3.6 \pm 0.4) \times 10^{-4}$ and $(3.6 \pm 1.0) \times 10^{-5}$ were determined for $\overline{p}d$ annihilation at rest into $K_S^0 K_L^0 n_{spectator}$ and $K_S^0 K_S^0 n_{spectator}$, respectively. The large uncertainty in the latter case is due to poor statistics for this channel which requires the $\overline{p}p$ subsystem to annihilate in the P-state. In the present data these reactions give rise to prominent groups of (i) 29 000 events and (ii) 1950 events selected in a similar fashion as above, but selecting for $\pi^+\pi^-$ pairs instead of $p\pi^-$. No cut on spectator momentum was applied. The results are not affected by neutron interaction in the barrel. In case (ii) where the momentum distribution of the neutron extends to rather large values [16] no cut on ESUM was required. In case (i) no significant dependence of the rates on the ESUM cut was found.

The acceptances of the detector and of the selection were determined by means of Monte Carlo simulations. These include a K^0_L interaction probability in the CsI barrel of 0.50±0.075 for K^0_L mesons of about 1100 MeV/c from the present Pontecorvo channels which was extrapolated from data (see [17]). Separate analyses for interacting and for noninteracting K^0_L mesons in the $K^0_S K^0_L n_{spectator}$ normalisation channel yielded consistent results. Total acceptances of about 20% (12%) were obtained for the Pontecorvo channels in the two-prong (four-prong) case. Very similar values were obtained for the normalisation channels in both cases. Hence the deduced annihilation rates are rather insensitive to uncertainties in the acceptances.

The $\overline{p}d$ annihilation rates (= branching ratios) into the Pontecorvo channels, given in Table 1, are obtained from the numbers of events by normalisation to the channels (i) and (ii), respectively, taking into account the acceptances and the known branching ratios [18] for the charged decay modes of Λ and K^0_S. Systematic errors are essentially due to uncertainties on the K^0_L interaction probability and on the branching ratios for the normalisation channels. The latter uncertainty is rather large in the 4-prong case as pointed out above, but it cancels in the ratio $R_{\Sigma^0\Lambda}$ of the branching ratios for the two Pontecorvo channels (Table 1). Comparing the results from the 2-prong and the 4-prong data, involving noninteracting K^0_L and K^0_S decaying into $\pi^+\pi^-$, respectively, agreement within errors is found for both $\overline{p}d \rightarrow \Lambda K^0$ and $\overline{p}d \rightarrow \Sigma^0 K^0$.

Table 2 summarises our branching ratios for the two Pontecorvo reactions by averaging the error-weighted branching ratios for the K^0_S and K^0_L modes of Table 1 and by multiplying the results with a factor of 2 to account for both observation modes of the K^0.

Comparison of our results with theoretical predictions (Table 2) based on the different models for the reaction mechanism quoted in the beginning, yields a rather clear picture. In the dynamical (two-step) model the rates of the open-strangeness channels turn out far too low. In particular the rates relative to $\overline{p}d \rightarrow p\pi^-$ are an order of magnitude or more below the experimental value of 20%. It was pointed out that these relative rates are less dependent on adjustable parameters than the absolute rates [2,19]. An alternative two-step calculation [4], including initial P-state annihilation and intermediate $\overline{K}^*$ exchange, shows a similar disagreement with the data.

Most striking is the two-orders of magnitude difference between the experimental and the two-step model values of the relative rate $R_{\Sigma^0\Lambda}$ of the two channels with open strangeness (Table 2). A strong suppression of ΣK with respect to ΛK^0 is fundamental to this model [2]. Strangeness conservation demands an intermediate $\overline{K}$ meson (or $\overline{K}^*$, see[4]) to be produced along with the K meson in the first step. In the second step, $\overline{K}N \rightarrow \Lambda$ is strongly enhanced as compared to $\overline{K}N \rightarrow \Sigma$, due to the larger isospin I=0 $\overline{K}$-nucleon-hyperon coupling strength compared to I=1. This difference, known from KN scattering, is related to the existence of the close-to-threshold spin 1/2 resonance $\Lambda(1405)$ [12,20]. A $\overline{\mathrm{p}}$d branching ratio for ΣK above 10^{-7} was considered to be beyond reach of the meson exchange mechanism [2]. A drastic increase of the coupling strength would be needed to reproduce our measurement by this approach.

Similar conclusions are obtained in the Regge model approach [7]. Including higher order exchange processes, the approach is intermediate between the two-step and the statistical model. While the predicted absolute values for the rates are somewhat larger than in the simple two-step model [2], relative rates of 10^{-3} for $\Sigma^0\mathrm{K}^0$ with respect to $\mathrm{p}\pi^-$ and of 0.04 with respect to $\Lambda\mathrm{K}^0$ ($=R_{\Sigma^0\Lambda}$) are expected [7], far below our experimental values.

The fireball model [5,6] assumes coalescence of the 9 participant quarks and antiquarks in a large quark bag with baryon number B=1 and the subsequent statistical evaporation into mesons and baryons. This process on the quark level is analogous to compound nuclear reactions on the nucleonic level. For the case of $\overline{\mathrm{p}}$-nucleus interactions, it was speculated that the B=1 fireball forms the seed of a quark-gluon plasma phase [5]. Strangeness enhancement, with respect to expectations of dynamical models, and almost equal Λ and Σ^0 rates are distinctive features of the fireball. Cugnon and Vandermeulen [6] expressed the rates in terms of a product of the B=1 fireball formation probability $P_{B=1}$ and of a phase space factor, evaluated for the final hadronic phase. Values of a few percent were estimated for $P_{B=1}$ in a simple geometrical picture [6]. As read from Table 2, with $P_{B=1}$=(2-3)% a good description of the data is achieved. Independent of this parameter, the relative rate $R_{\Sigma^0\Lambda}$ is in perfect agreement with the data.

In conclusion, the present discovery of open strangeness Pontecorvo reactions on deuterium was accomplished by independent analyses of the K^0_S and the K^0_L modes of the $\Lambda\mathrm{K}^0$ and $\Sigma^0\mathrm{K}^0$ channels. Rather clean event samples were selected without any kinematic fitting and $\overline{\mathrm{p}}$d branching ratios close to 2×10^{-6} were deduced for both channels. These rates and, in particular, the relative rate $R_{\Sigma^0\Lambda}$ exceed by far the values expected from two-step models. With the present understanding of meson - baryon interaction, this finding means that the simple meson exchange picture is inadequate to describe these Pontecorvo reactions [2,4,7,19]. On the other hand, our observations agree with predictions for the parton fireball [6]. They can be taken as evidence that the original nucleonic quark bags dissolve into a large bag with baryon number B=1.

We would like to thank the technical staff of the LEAR machine group and of all the participating institutions for their invaluable contributions to the success of the experiment. We acknowledge financial support from the German Bundesministerium für Bildung, Wissenschaft, Forschung und Technologie, the Schweizerischer Nationalfonds, the British Particle Physics and Astronomy

Research Council, the U.S. Department of Energy and the National Science Research Fund Committee of Hungary (contract No. DE–FG03–87ER40323, DE–AC03–76SF00098, DE–FG02-87ER40315 and OTKA F014357). K. M. C., N. D., F. H. H. and R.O. acknowledge support from the Alexander von Humboldt Foundation.

References

[1] B.M. Pontecorvo, Sov.Phys. JETP **3** (1956) 966

[2] L.A. Kondratyuk and M.G. Sapozhnikov, Phys. Lett. **B220** (1989) 333

[3] L.A. Kondratyuk and C. Guaraldo, Phys. Lett. **B256** (1991) 6

[4] E. Hernandez and E. Oset, Phys. Lett. **B226** (1989) 223

[5] J. Rafelski, Phys.Lett. **B91** (1980) 281, **B207** (1988) 371

[6] J. Cugnon and J. Vandermeulen, Phys. Lett. **B146** (1984) 16 and Phys. Rev. **C39** (1989) 181

[7] A.B. Kaidalov, Sov.J.Nucl.Phys. **53** (1991) 872

[8] R. Bizzari et al., Lett Nuovo Cimento **2** (1969) 431

[9] V.G. Ableev et al., Obelix Collaboration, Nucl.Phys. **A562** (1993) 617

[10] C. Amsler et al., Crystal Barrel Collaboration, Z.Phys. **A351** (1995) 325

[11] C. Amsler et al., Crystal Barrel Collaboration, Phys.Lett. **B352** (1995) 187; O. Denisov et al., Obelix Collaboration, Phys. Lett. **B460** (1999) 248

[12] R.H. Dalitz, Annals of Physics **3** (1960) 307

[13] E. Aker et al., Crystal Barrel Collaboration, NIM **A321** (1992) 69

[14] M. Doser et al., NIM **A412** (1998) 70; C. Regenfus, NIM **A386** (1997) 60

[15] C. Regenfus, Ph.D.thesis, Universität München, 1997 and Proc. LEAP 98, Nucl. Phys. **B**(in press)

[16] R. Bizzari et al., Nucl. Phys. **B69** (1974) 307

[17] A. Abele et al., Crystal Barrel Collaboration, Phys. Rev. **D57** (1998) 3860

[18] Particle Data Group, Eur. Phys. J. **C** 3(1998) 1

[19] D.E. Kharzeev, F. Nichitiu and M.G. Sapozhnikov, Sov. J. Nucl. Phys. **55** (1992) 748

[20] J.M. Eisenberg and D.S. Koltun, Theory of Meson Interactions with Nuclei (Wiley, New York, 1980)

channel	observed mode	events	BR $[10^{-6}]$
ΛK^0_L	$\Lambda \to p\pi^-$, K^0_L(noninteracting)	$107 \pm 11 \pm 6$	$1.1 \pm 0.1 \pm 0.2$
$\Sigma^0 K^0_L$	$\Sigma^0 \to \Lambda\gamma$, $\Lambda \to p\pi^-$, K^0_L(noninteracting)	$83 \pm 10 \pm 9$	$1.0 \pm 0.1 \pm 0.2$
			$R_{\Sigma^0\Lambda} = 0.90 \pm 0.13 \pm 0.13$
ΛK^0_S	$\Lambda \to p\pi^-$, $K^0_S \to \pi^+\pi^-$	$85 \pm 10 \pm 10$	$1.6 \pm 0.3 \pm 0.5$
$\Sigma^0 K^0_S$	$\Sigma^0 \to \Lambda\gamma$, $\Lambda \to p\pi^-$, $K^0_S \to \pi^+\pi^-$	$61 \pm 8 \pm 5$	$1.5 \pm 0.2 \pm 0.5$
			$R_{\Sigma^0\Lambda} = 0.95 \pm 0.17 \pm 0.16$

Table 1
Observed event numbers after background subtraction, deduced $\bar{p}d$ *annihilation rates at rest ("branching ratios"* BR*) and relative branching ratios* $R_{\Sigma^0\Lambda} = BR(\Sigma^0 K^0)/BR(\Lambda K^0)$*. The first errors give the statistical uncertainties (1σ), the second the systematic uncertainties.*

(i) Absolute $\overline{\text{p}}$d branching ratios (BR) [10^{-6}]

	experimental	dyn. model [2]	dyn. model [4]	stat. model [6]
ΛK^0	2.35 ± 0.45^a	0.3		$1.0 \times P_{B=1}{}^c$
$\Sigma^0 K^0$	2.15 ± 0.45^a	0.004	0.01 - 0.025	$1.0 \times P_{B=1}{}^c$
$p\pi^-$	13.0 ± 1.0^b	2 - 6	38	$4.7 \times P_{B=1}{}^c$

(ii) Relative branching ratios $R_{\Sigma^0\Lambda} = BR\,(\Sigma^0 K^0)\,/\,BR\,(\Lambda K^0)$

	experimental	dyn. model [2]		stat. model [6]
	0.92 ± 0.15^a	0.012		1.0

[a] Weighted average of the results in Table 1 with quadratically added statistical and systematic errors.

[b] Weighted average of the results of Ref. 9 and 10, applying charge independence to the $n\pi^0$ result [10]

[c] Total probability [%] of forming a fireball with baryon number B=1. Estimates yield $P_{B=1} \lesssim 10\,\%$ (Ref.[6]).

Table 2

Comparison of experimental results and predictions of dynamical and statistical models

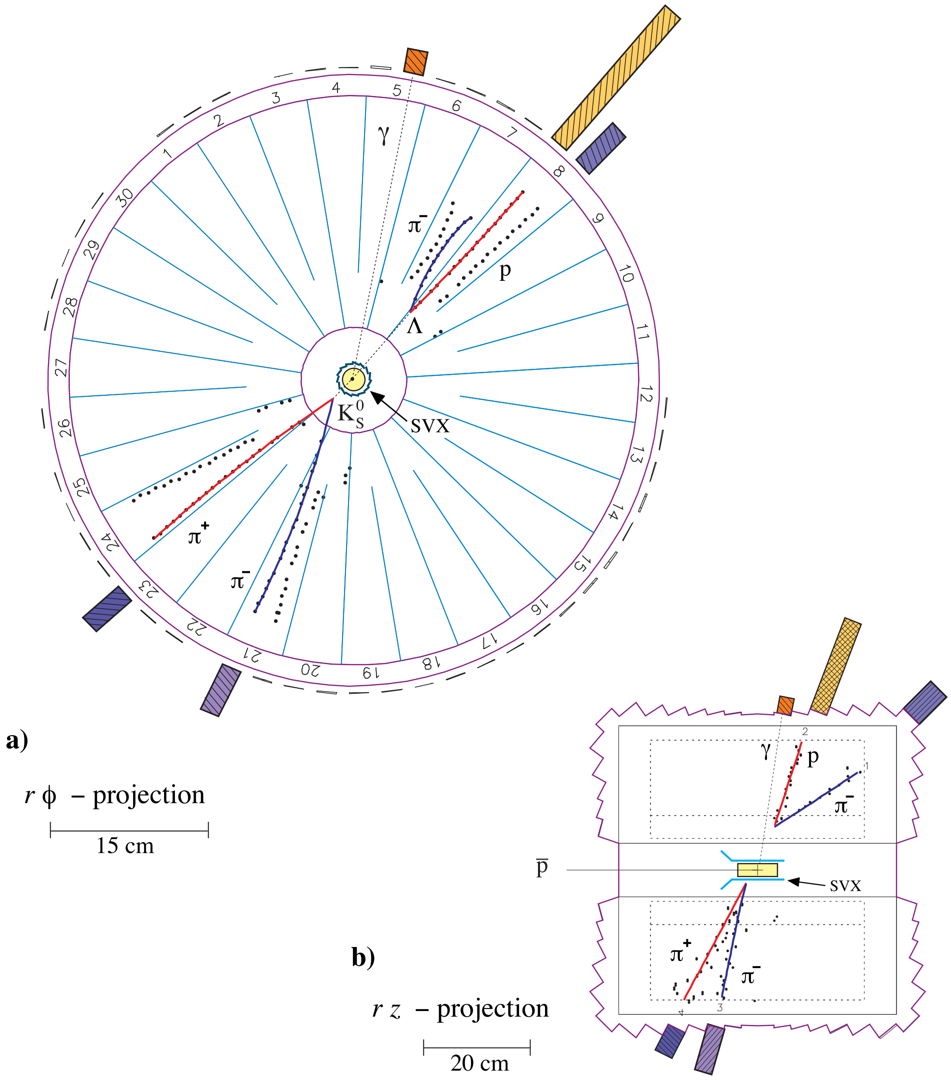

Fig. 1. Event of the Pontecorvo type, selected from the data set. With the charged-particle multiplicities 0 in the SVX and 4 in the drift chamber, it shows the complete signature of a $\overline{\mathrm{p}}\mathrm{d}\to\Sigma^0\mathrm{K}^0_\mathrm{S}$ *(*$\Sigma^0\to\Lambda\gamma$*,* $\Lambda\to\mathrm{p}\pi^-$*,* $\mathrm{K}^0_\mathrm{S}\to\pi^+\pi^-$*) event in the transverse (a) as well as in the longitudinal projections (b). The apparent left-right ambiguity of hits in the drift chamber is resolved (full line trajectories) by the sense wire staggering [13]. Clockwise and anticlockwise curvatures in a) correspond to negative and positive charges, respectively. Energy deposits in the barrel-shaped electromagnetic calorimeter are represented by bars of proportional lengths.*

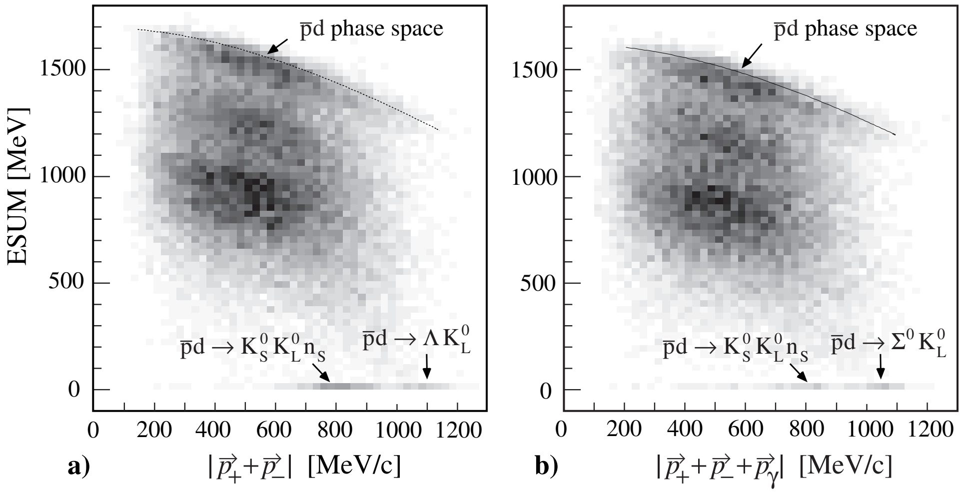

Fig. 2. a) Sum of energy deposits from photons in the electromagnetic calorimeter (ESUM) versus the total momentum of the positively and the negatively charged particles for all 2-prong events that passed the preselection criteria for $\Lambda \rightarrow p\pi^-$ decays given in the text. b) Analogous representation of the subset satisfying the preselection criteria for $\Sigma^0 \rightarrow \Lambda\gamma$ ($\Lambda \rightarrow p\pi^-$) decays. Here the photon attributed to this decay is excluded from ESUM.

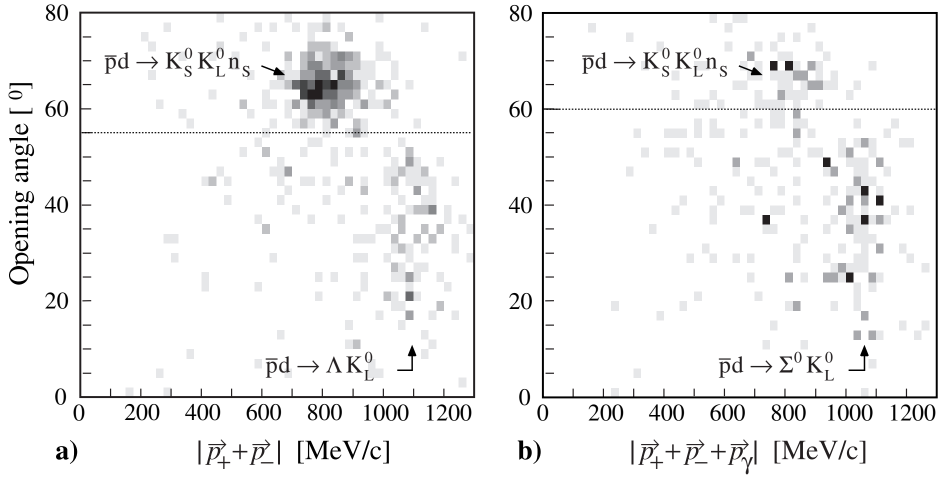

Fig. 3. Two-prong opening angle (lab system) versus momentum for the preselected events containing a) two charged particles and b) two charged particles and a photon, but no residual energy deposit ESUM in the calorimeter (see Fig. 2). Events containing $\Lambda \rightarrow p\pi^-$ *decay are selected by the indicated cuts on the maximum opening angle. Background from* $\overline{p}d \rightarrow K_S^0$ *(*$\rightarrow \pi^+\pi^-$*)* K_L^0(noninteracting) $n_{spectator}$ *is identified at opening angles around 65°.*

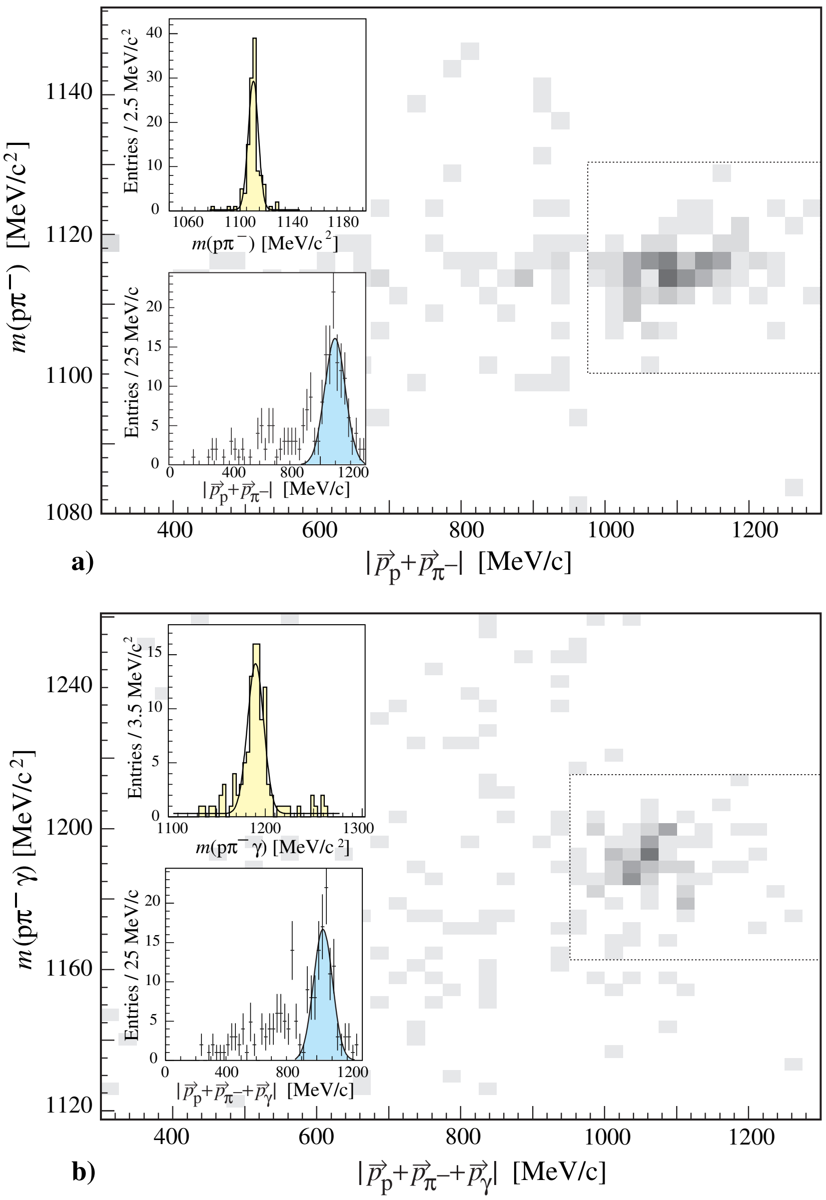

Fig. 4. a) Invariant mass versus total momentum for the $\mathrm{p}\pi^-$ *pairs selected from Fig. 3a. The insets show the projections on both axes and Gaussian fits, yielding* $m(\mathrm{p}\pi^-) = 1116\,\mathrm{MeV/c^2}$, $\sigma = 4\,\mathrm{MeV/c^2}$ *and* $p = 1099\,\mathrm{MeV/c}$, $\sigma = 68\,\mathrm{MeV/c}$. *The dotted box indicates the final selection of* $\overline{\mathrm{p}}\mathrm{d}\to\Lambda\mathrm{K^0_L}$(noninteracting) *events. b) Invariant mass versus total momentum for the* $\mathrm{p}\pi^-\gamma$ *combinations, selected from Fig. 3b, and projections with Gaussian fits, yielding* $m(\mathrm{p}\pi^-\gamma) = 1190\,\mathrm{MeV/c^2}$, $\sigma = 8\,\mathrm{MeV/c^2}$ *and* $p = 1043\,\mathrm{MeV/c}$, $\sigma = 62\,\mathrm{MeV/c}$. *The dotted box indicates the final selection of* $\overline{\mathrm{p}}\mathrm{d}\to\Sigma^0\mathrm{K^0_L}$(noninteracting) *events.*

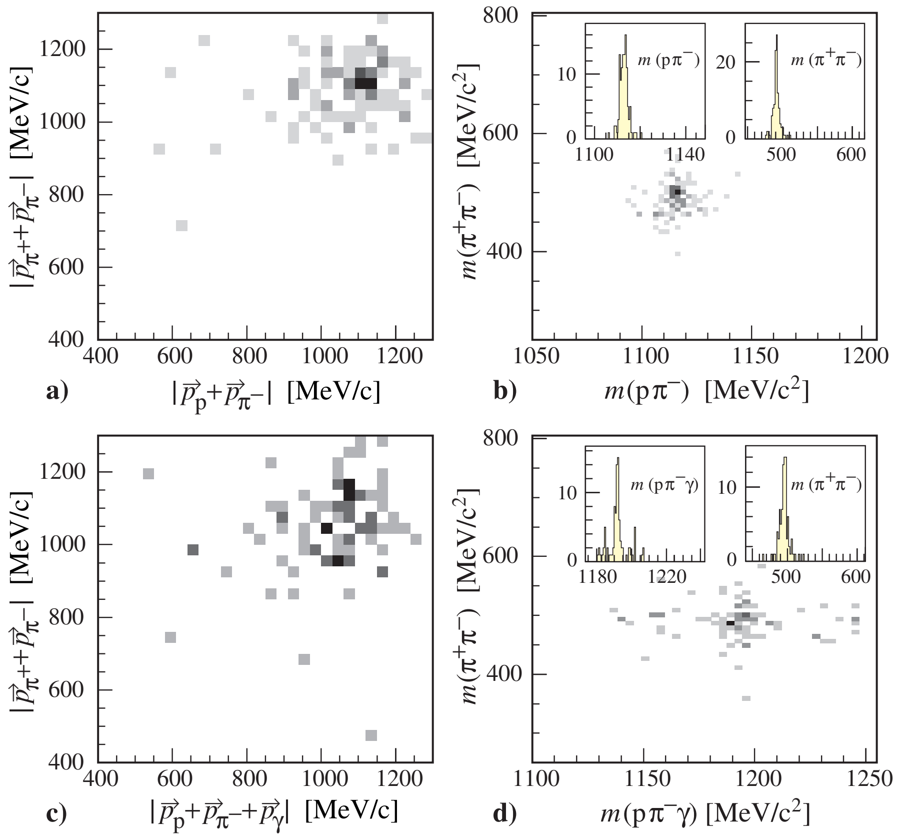

Fig. 5. Four-prong events with secondary $\pi^+\pi^-$ and $\mathrm{p}\pi^-$ vertices and with zero (a,b) or one (c,d) photon. The two-body channel $\overline{\mathrm{p}}\mathrm{d}\to\Lambda\mathrm{K}^0_\mathrm{S}$ with subsequent $\Lambda\to\mathrm{p}\pi^-$ and $\mathrm{K}^0_\mathrm{S}\to\pi^+\pi^-$ decays is identified in the distribution of the total momentum of the $(\pi^+\pi^-)$ pair versus the total momentum of the $(\mathrm{p}\pi^-)$ pair (a) or of one invariant mass versus the other (b). The primary two-body channel $\overline{\mathrm{p}}\mathrm{d}\to\Sigma^0\mathrm{K}^0_\mathrm{S}$ with subsequent $\Sigma^0\to\Lambda\gamma$ $(\Lambda\to\mathrm{p}\pi^-)$ and $\mathrm{K}^0_\mathrm{S}\to\pi^+\pi^-$ decays is identified in the distribution of the total momentum of the $(\pi^+\pi^-)$ pair versus the total momentum of the $(\mathrm{p}\pi^-\gamma)$ system (c), or of the corresponding invariant masses (d). The insets show projections on the respective invariant mass axes.